JOURNAL OF MASS SPECTROMETRY, VOL. 33, 75–84 (1998)

Probing the Energetics of Charge-remote Fragmentation in Carbocyanine Dyes Using Collision- and Surface-induced Dissociation Mass Spectrometry

Michael C. Melnyk,[1] Richard E. Carlson,[1] Kenneth L. Busch,[1]* Kevin L. Schey[2] and Michael G. Bartlett[3]

[1] School of Chemistry and Biochemistry, Georgia Institute of Technology, Atlanta, Georgia 30332-0400, USA

[2] Department of Cell and Molecular Pharmacology, Medical University of South Carolina, Charleston, South Carolina 29425-2251, USA

[3] Department of Medicinal Chemistry, University of Georgia, Athens, Georgia 30602-2352, USA

Carbocyanine dyes used as molecular probes are symmetric ring compounds with long alkyl chains on each ring proximate to a resonance-stabilized charge site. They provide high-quality positive-ion liquid second (LSI) and electrospray ionization mass spectra in which the intact cation is the dominant ion in the mass spectrum. The intact cation of a carbocyanine dye undergoes charge-remote fragmentation (CRF), evident in the LSI mass spectra. CRF is also observed in collision-induced dissociation and surface-induced dissociation of the mass-selected intact cation. Differential CRF processes from the two chains in the molecule are observed with increasing internal energy deposition. © **1998 John Wiley & Sons, Ltd.**

J. Mass Spectrom. **33**, 75–84 (1998)

KEYWORDS: liquid secondary ion mass spectrometry; charge-remote fragmentation; electrospray; carbocyanine dyes

INTRODUCTION

Charge-remote fragmentation (CRF)[1] has been used to identify the branching points or double bond location in compound classes such as fatty acids,[2,3] alkylammonium salts[4] and bile acids.[5] Typically, charge-remote fragmentation is observed following collision-induced dissociation (CID).[1,4,6] The amount of energy required to promote CRF[4,7,8] appears to be both compound dependent and related to the inherent stability of the charge site.[5] Two different mechanisms have been suggested for CRF: the 1,4-elimination mechanism, suggested by Gross and co-workers,[2,7] and a radical mechanism resulting in the formation of a distonic ion, proposed by Wysocki and Ross.[14]

We have shown previously[9] that substituted carbocyanine dyes exhibit a CRF process in their liquid secondary ion mass spectra. In this paper we show that the CRF process also occurs for these compounds in collision-induced dissociation (CID) for both electrospray ionization (ESI) and liquid secondary ion mass spectrometry (LSIMS) and surface-induced dissociation (SID) following LSIMS, and we compare the energy dependences of these processes.

* Correspondence to: K. L. Busch, School of Chemistry and Biochemistry, Georgia Institute of Technology, Atlanta, Georgia 30332-0400, USA, kenneth.busch@chemistry.gatech.edu

CCC 1076–5174/98/010075–10 $17.50

Received 16 May 1997
Accepted 8 October 1997

The structural feature that promotes CRF fragmentation in these molecules is the presence of two long alkyl chains proximate to a resonance-stabilized charge site. The dyes studied in this work are divided into two groups; those containing (structures **I–IV**) and those lacking (structures **V–VII**) a second heteroatom in the indole ring, as shown in Figs 1 and 2, respectively. The presence of two alkyl chains in these molecules, and the chance to form different series of ions formed by sequential CRF processes, allow a unique probe of the energies of the CRF process. The relative energies of energy deposition in CID and SID can be explicitly compared through investigation of the extent of CRF processes as a function of parameters of the CID and SID experiments. In this paper, we focus on the dissociations of three dyes chosen specifically to reveal differences in CRF dissociation processes with varying internal energy deposition, although data were recorded for all the dyes shown in Figs 1 and 2.

EXPERIMENTAL

Instrumentation

Positive ion LSIMS and low-energy (<250 eV) CID experiments were performed on a VG 70-SEQ hybrid mass spectrometer of EBqQ geometry. (VG Analytical, Manchester, UK). Positive ion ESI and low-energy (<100 eV) CID experiments were performed on a VG

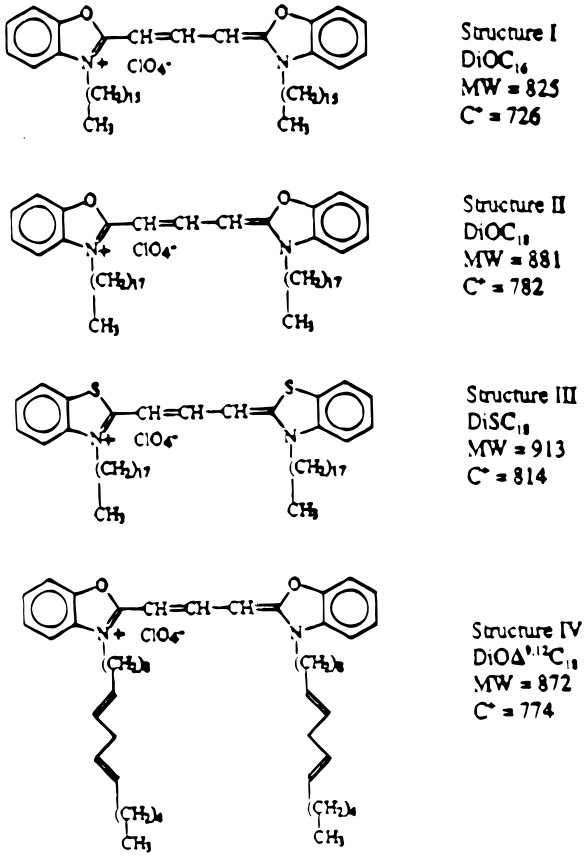

Figure 1. Carbocyanine dyes **I–IV**.

Quattro II triple quadrupole mass spectrometer. High-energy CID and SID experiments were performed on a JEOL HX110/HX110 mass spectrometer of EBEB geometry. Both the VG70-SEQ and the JEOL HX110/HX110 instruments used a cesium ion beam to sputter ions from sample solutions prepared in neat *m*-nitrobenzyl alcohol (*m*-NBA) (Aldrich, Milwaukee, WI, USA). Air and helium were used as collision gases, and the acceleration voltages were 8000 and 10 000 V on the VG70-SEQ and JEOL instruments, respectively. The precursor ion beam signal was attenuated by ~50% and ~70% in the low- and high-energy CID experiments, respectively. The collision energy (laboratory reference frame) was varied from 250 to 9.75 keV for energy-resolved MS/MS studies. SID was investigated on a perfluoropolyether (Krytox 1625, DuPont, Wilmington, DE, USA)-coated brass surface[10] and the collision energies used were 75, 100, 150, 200 and 300 eV. The SID device was placed in the collision cell region of the JEOL mass spectrometer as described.[10] In all cases, at least unit mass resolution selection of the parent ion beam was achieved. A VAX-based computer system and OPUS 3.0 software were used to acquire and process data on the VG70-SEQ instrument. JEOL Complement software was used to process and acquire the data on the HX110 instrument. The data system for the VG Quattro II triple quadrupole mass spectrometer was MassLynx version 2.22. Sample concentrations of solutions used in electrospray experiments were ~20 pmol μl^{-1}. The needle voltage was 3500–3700 V, the cone voltage was 70–80 V and the source temperature was ~80 °C. In MS/MS CID for electrospray ionization, the collision gas was 99.999% argon. The collision energies ranged from 5 to 100 eV. The collision cell pressure was $\sim 1.5 \times 10^{-3}$ Torr (1 Torr = 133.3 Pa), corresponding to a parent ion beam attenuation of 50%. Unit mass resolution selection of parent ions was again achieved.

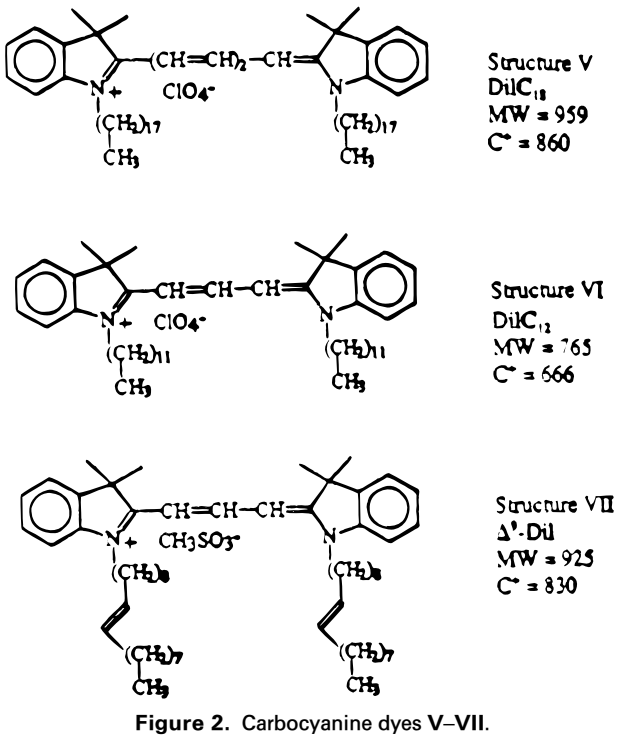

Figure 2. Carbocyanine dyes **V–VII**.

Methods

A dry layer of CsI or a glycerol film was sputtered from the probe to calibrate the mass scale for the VG 70-SEQ and JEOL instruments. Dyes were purchased from Molecular Probes (Eugene, OR, USA) and used as received. All LSI mass spectra were measured from dye solutions prepared in neat *m*-NBA. All ESI mass spectra were measured from dye solutions prepared in 1:1 methanol–acetonitrile. For LSIMS data, ion signals were recorded for 3–5 min, or 50–90 scans, and the spectra were averaged. In ESI experiments, samples were injected using a Kd Scientific Model 200 syringe pump at a flow-rate of 10 $\mu l\ min^{-1}$. Mass spectra were obtained using the MCA mode and represent the average of 15–20 scans. The mass range of 100–1500 Da was scanned at a rate of 6 s per scan.

DISCUSSION

The dyes discussed in this paper contain two long alkyl or alkenyl chains proximate to a resonance-stabilized charge site. In the following discussion, 'first' alkyl (or alkenyl) chain processes refer to fragmentations that produce ions between the *m/z* of the intact cation (or

precursor ion) and the *m/z* corresponding to complete loss of one of the alkyl or alkenyl chains. 'Second' chain refers to fragment (or product) ions resulting from losses originating in the remaining alkyl chain. For example, the mass spectrum of $DiSC_{18}$ (**I**) contains an intense signal corresponding to the intact cation at *m/z* 814. Loss of one complete alkyl chain in this compound produces a fragment ion at *m/z* 561; this represents loss of the first alkyl chain. Loss of all of the remaining alkyl chain produces a fragment ion at *m/z* 307.

Mass spectrometry

LSI mass spectra. We begin with a brief summary of the positive ion LSI mass spectra of these compounds, concentrating on CRF processes. A more detailed discussion is given elsewhere.[9] $DiSC_{18}$, $DiO\Delta^{9,12}C_{18}$ and $DilC_{18}$ were chosen as representative examples of this class of compounds (**I**, **IV** and **II**). Figure 3 shows a portion of the positive ion LSI mass spectrum of $DiSC_{18}$ (**I**) in the region between *m/z* 250 and 850, containing ions that correspond to charge-remote fragmentation of the first alkyl chain. The intact cation of the dye appears at *m/z* 814, and fragments to form the ion at *m/z* 561 by complete loss of the first chain. A fragment ion at *m/z* 798 corresponds to loss of CH_4 from the intact cation; the ion at *m/z* 786 is believed to be an impurity in the original dye, as this ion was absent in product ion MS/MS experiments for the intact cation. First chain CRF fragments are a series of ions separated by 14 Da, terminating at *m/z* 561 by a final mass separation of 13 Da. Associated with each CRF fragment ion (separated by 14 Da) is a group of adjacent, usually lower abundance ions. As an example, the ion at *m/z* 758 (formally, loss of 56 Da from the intact cation) is accompanied by a slightly higher abundance ion at *m/z* 756 and lower abundance ions at *m/z* 757 and 759. There is a small contribution from background noise from the *m*-NBA matrix, but the majority of the signal is genuinely associated with the CRF fragment ions. This can be seen in the reproducible pattern observed for the cluster of ions observed around each CRF product ion. This pattern suggests a series of common mechanisms involving hydrogen transfer reactions that accompany each CRF. Excellent pattern reproducibility is seen in the cluster of ions around the CRF fragment ions at *m/z* 686, 672, 658, 643 and 629. These CRF losses correspond to a C_nH_{2n+2} and/or a C_nH_{2n+1} series as suggested by Adams and Gross[7] and Wysocki and Ross,[4] respectively. Finally, a loss of neutral thiophenol from the intact cation at *m/z* 814 results in the fragment ion at *m/z* 705. The mass spectrum in Fig. 3 is representative of the quality of the LSI mass spectra obtained for each of the carbocyanine dyes. Second chain CRF ions were not observed in the LSI mass spectra of any of these carbocyanine compounds.

The mass spectrum of $DiO\Delta^{9,12}C_{18}$, a compound with two double bonds in each of the alkyl chains, is also characterized by first loss of neutral CH_4 from the intact cation at *m/z* 774, followed by a series of four peaks separated again by 14 Da, until the position of the double bond is reached. At the point of the double bond, the abundance of the CRF fragment ion is diminished and the fragment ion separation becomes 12 Da. After this point, the normal CRF fragment ion (separation of 14 Da) continues until the next double bond in the chain is reached, indicated again by a loss

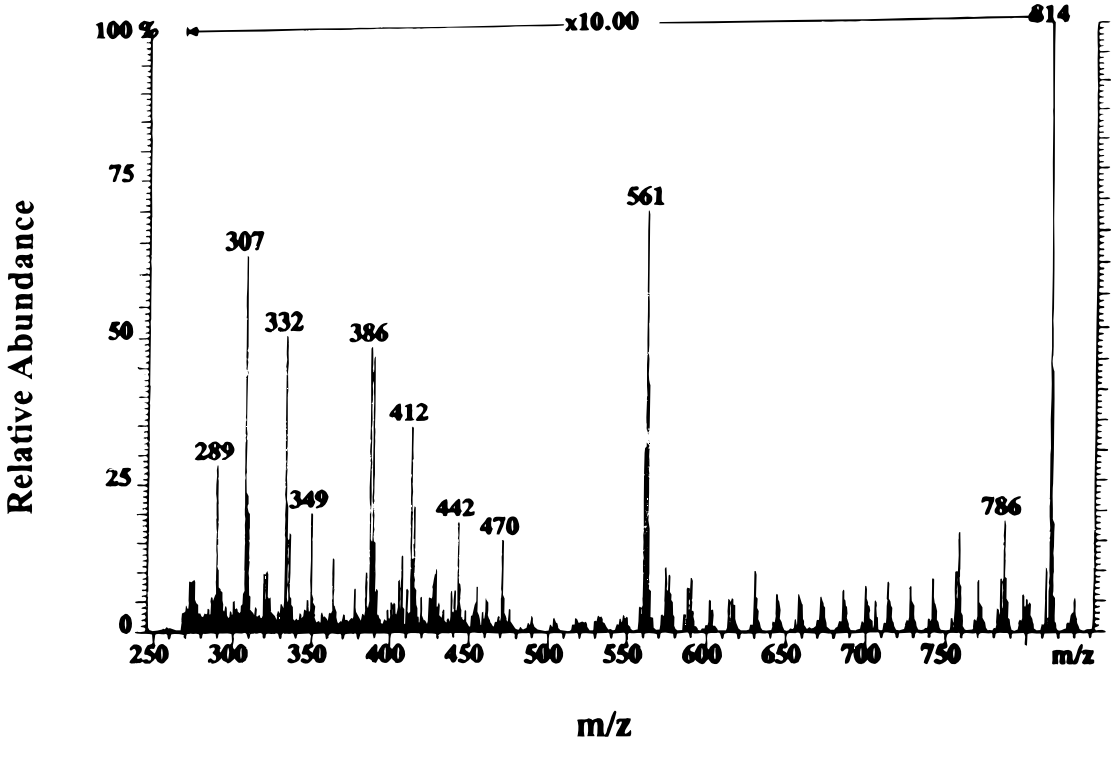

Figure 3. Positive ion LSI mass spectrum of $DiSC_{18}$ showing the region from *m/z* 250 to 850.

of 12 Da, and lower intensity signal. Fragment ions corresponding to a C_nH_{2n+2} series (separation of 14 Da) were observed for the loss of one entire side-chain. Initial loss of CH_4 from the intact cation is consistent with a radical ion-based CRF mechanism as proposed by Wysocki and Ross.[4] Loss of methane from the intact cations of both $DiSC_{18}$ and $DiO\Delta^{9,12}C_{18}$ may also be explained by hydrogen transfer from the neighbouring alkyl group to the terminal alkyl group first lost. Hydrogen transfer may be repeated along the alkyl (or alkenyl) chain until the final alkyl group is cleaved. This hydrogen transfer mechanism is not entirely consistent with the mechanisms suggested by Adams and Gross[7] and Wysocki and Ross[4] and is under further investigation.

Finally, LSI mass spectrum of $DilC_{18}$ exhibits two consecutive losses of 15 Da (*m/z* 845 and 830) from the intact cation at *m/z* 860, followed again by a series of peaks separated by 14 Da, terminating at the ion at *m/z* 606, corresponding to the complete loss of one alkyl side-chain. The successive losses of 15 Da may result from the loss of each of the two terminal methyl groups on the alkyl chains, after which charge-remote fragmentation occurs for each chain. A putative radical site at the end of each of the two alkyl chains initiates the CRF processes. The LSI mass spectra of the other carbocyanine dyes are similar to that of $DilC_{18}$ with the analogous losses of two methyl groups, which suggests that the first methyl group loss is from the ring rather than from the alkyl chain.

ESI mass spectra. The sputtering process in LSIMS provides cations with sufficient energy to initiate the CRF process.[9] Our focus now turns to ESIMS. Here the cations are produced with a very low internal energy and the amount of dissociation (including CRF) should be minimal. Positive ion ESI mass spectra were recorded; two representative examples of carbocyanine dyes are chosen for discussion: $DiSC_{18}$ and $DilC_{12}$. Figure 4 shows a portion of the positive ion ESI mass spectrum of $DiSC_{18}$. As expected, the amount of fragmentation is minimal and the intact cation dominates the mass spectrum. Examination of the mass region between *m/z* 550 and 810 shows that there is no charge-remote fragmentation of the first chain, as was seen in the LSI mass spectrum (Fig. 3). For each of the carbocyanine dyes examined by ESI, there is very little fragmentation in the mass spectrum. In the positive ion ESI mass spectrum of $DilC_{12}$, the intact cation appears at *m/z* 666, complete loss of the first alkyl chain results in the signal at *m/z* 495, but there is no evidence of CRF. The abundant cation obtained in ESI is therefore an ideal candidate for MS/MS studies, which are described in a later section.

MS/MS results

High-energy collision-induced dissociation. Attention now turns to CRF processes initiated by ion activation, particularly CID. Figure 5 shows a portion of the CID tandem mass spectrum of the intact cation of $DiSC_{18}$ at *m/z* 814 recorded on the JEOL HX110/HX110 mass spectrometer. The collision energy in the laboratory frame of reference was 7.0 keV. The tandem mass spectrum shown is representative of those obtained for each of the dyes in Fig. 1. As in the LSIMS data, the fragmentation includes initial loss of CH_4 from the cation,

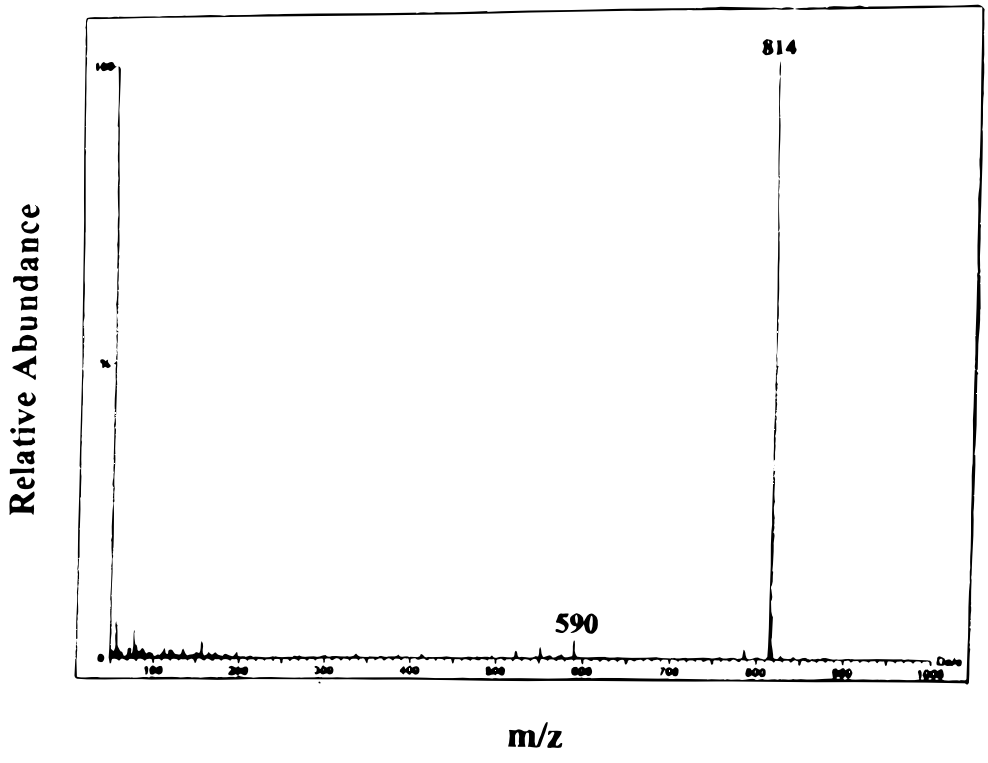

Figure 4. Positive ion ESI mass spectrum of $DiSC_{18}$ showing the region from *m/z* 50 to 1000.

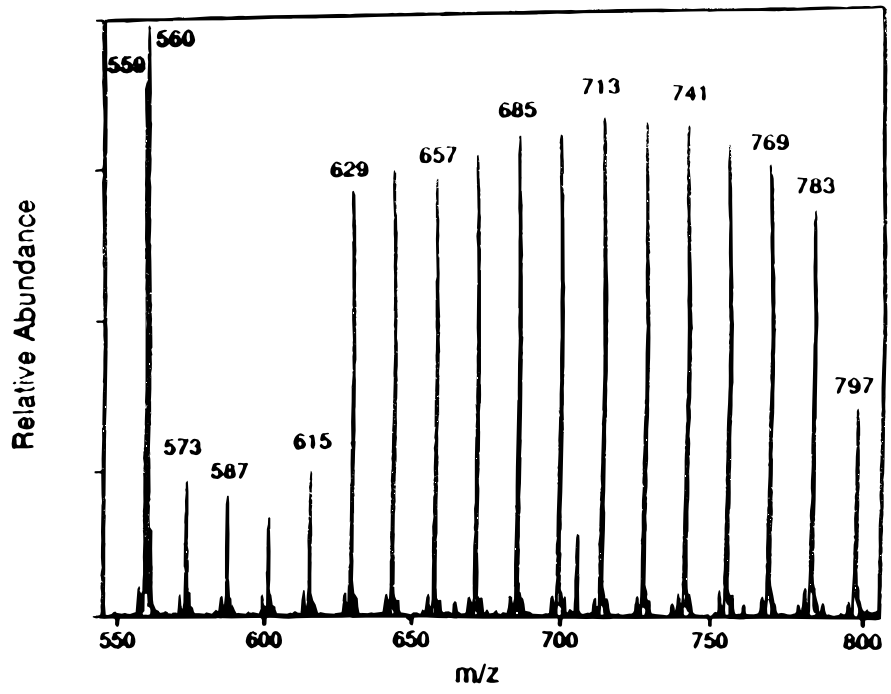

Figure 5. High-energy CID tandem mass spectrum of $DiSC_{18}$ at a collision energy of 7.0 keV in the region from *m/z* 550 to 805.

followed by a series of product ions separated by 14 Da, with the charge-remote losses of one alkyl chain terminating in the ion at *m/z* 561. These product ions in the C_nH_{2n+2} series are accompanied by lower abundance product ions that correspond to a C_nH_{2n+1} series. The product ion at *m/z* 705 again corresponds to loss of thiophenol. CRF losses along the second chain can be observed with lower signal intensities. At laboratory collision energies greater than 3.0 keV, CRF losses in *both* alkyl (or alkenyl) chains are observed in the CID tandem mass spectra of the dyes. As the collision energy dropped below 3.0 keV, losses were not observed for the second alkyl chain. However, the exact collision energy at which the second-chain CRF losses are no longer observed is compound dependent. First-chain CRF losses persist even at the low collision energies.

The CID tandem mass spectra (6.5 keV) of $DilC_{18}$ (a Fig. 2 dye) shows two successive losses of 15 Da (two CH_3 groups) from the intact cation at *m/z* 860, again followed by a series of product ions corresponding to CRF losses of ions in the C_nH_{2n+2} series. The product ions corresponding to CRF losses from within the second chain are lower in relative abundance. The high-energy CID tandem mass spectra for all Fig. 2 dyes are similar in that first-chain CRF fragment ions are distinct and the second-chain CRF ions are less abundant. Energy-resolved MS/MS in the high collision energy CID regime for these Fig. 2 dyes show that second-chain CRF does not occur at all below laboratory collision energies of 5.5 keV. With the same collision gas pressure, the dyes in Fig. 1 showed CRF in both chains at all laboratory collision energies greater than 3.0 keV.

Figure 6 is the high-energy CID spectrum for $DiO\Delta^{9,12}C_{18}$, recorded at a laboratory collision energy of 7.0 keV, and shown in the region from *m/z* 500 to 760. CRF in the first alkenyl chain is evident in this mass spectrum. Following neutral loss of CH_4 from the precursor ion at *m/z* 774 (the intact cation), four product ions separated by 14 Da are observed, with fragmentation continuing until the position of the double bond is reached. As before, the abundance of the fragment ions separated by 12 Da from adjacent product ions is reduced. This is the same pattern of altered ion abundances observed in the mass spectrum itself. After the double bond, the CRF fragmentation pattern resumes with ions within the C_nH_{2n+2} series until the next double bond in the chain is reached, indicated again by adjacent product ion separation of 12 Da, and diminished ion abundances. After the second double bond is passed, losses of ions within the C_nH_{2n+2} product ion series resume until loss of one entire side-chain is complete. CRF dissociation and loss of the second alkenyl chain are also observed under these high-energy CID conditions. The fragment ions corresponding to the position of the double bonds in the CRF fragmentation pattern are indicated by a label on the mass spectrum shown in Fig. 6.

Low-energy collision-induced dissociation. The occurrence of both first- and second-chain CRF fragmentations in high-energy CID has been demonstrated. Low collision energy CID can be expected to deposit a lower average amount of internal energy into the precursor ion, and may involve direct vibrational excitation rather than a two-step electronic/vibrational excitation. We therefore studied the lower energy CID process for these compounds, here investigated on the hybrid EBqQ mass spectrometer.

Figure 7 shows a portion of the low-energy CID tandem mass spectrum of $DiSC_{18}$ (**I**) recorded on a VG70-SEQ mass spectrometer at a laboratory collision energy of 40 eV. The precursor ion (not shown) is the intact cation at *m/z* 814. In contrast to the clear pattern of CRF fragment ions previously observed in the high-

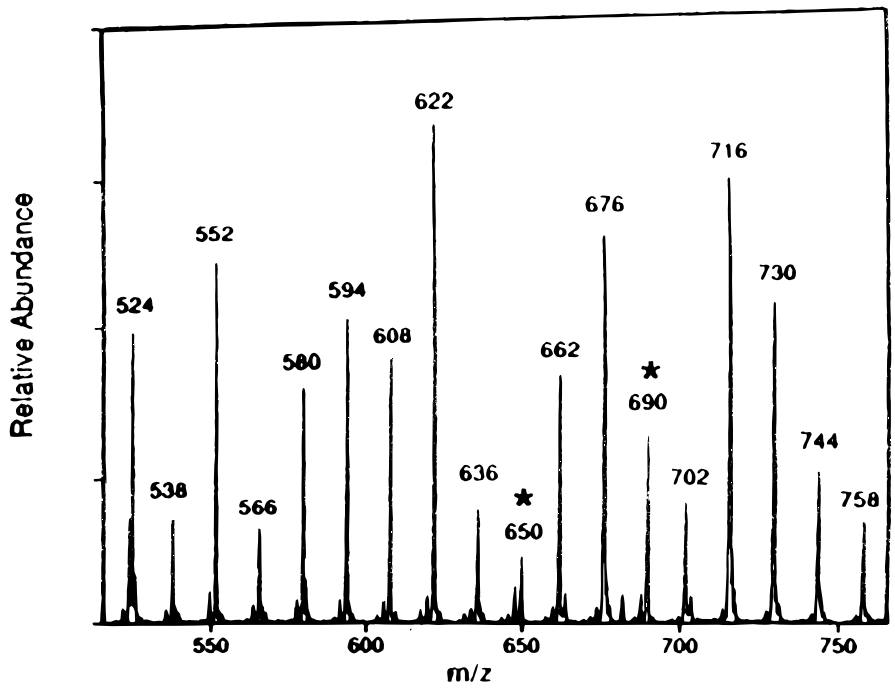

Figure 6. High-energy CID tandem mass spectrum of DiO$\Delta^{9,12}C_{18}$ at a collision energy of 7.0 keV in the region from *m/z* 500 to 760. Asterisks mark the fragment ions corresponding to the position of the double bonds in the CRF fragmentation pattern.

energy CID tandem mass spectrum, this spectrum is dominated by product ions at *m/z* 561, 412, 386, 309 and 173, all of which are unrelated to the CRF process. CRF ions corresponding to losses from within the first alkyl chain are absent. Some of the product ions corresponding to second-chain CRF dissociation are present in the low-energy tandem mass spectrum of $DiSC_{18}$. Nine of 18 possible CRF product ions corresponding to the C_nH_{2n+2} series are observed; ions in the C_nH_{2n+1} series are not observed. The ions at *m/z* 412 and 386 are also present in the LSI and high-energy tandem mass spectra of this compound. The high-energy tandem mass spectrum of $DiSC_{18}$ contains a product ion at *m/z* 307, proposed to be the dehydrogenation product of the

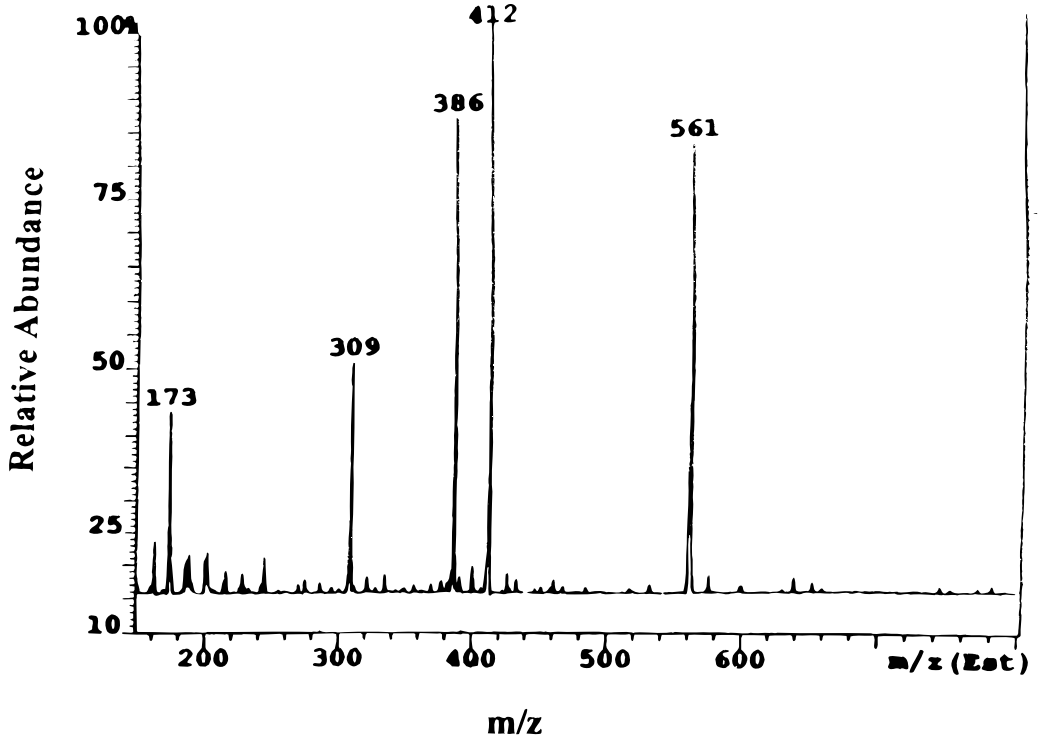

Figure 7. Low-energy CID tandem mass spectrum of $DiSC_{18}$ at a collision energy of 40 eV in the region from *m/z* 150 to 800.

fragment ion at *m/z* 309. Under low-energy CID conditions, only the fragment ion at *m/z* 309 is observed. All of the dyes in Fig. 1 exhibited similar behavior to $DiSC_{18}$ under low-energy CID MS/MS conditions.

The low-energy CID spectra of the dyes in Fig. 2 showed similar features to the low-energy CID spectrum of $DiSC_{18}$, with the exception of two consecutive losses of 15 Da from the precursor ion as noted in the LSI mass spectrum of $DilC_{18}$.

Surface-induced dissociation. SID has emerged as an alternative method for ion energization and dissociation.[10–14] The next step in this study was to determine how the results of SID experiments compare with both low- and high-energy CID with respect to the occurrence of CRF processes.

The SID tandem mass spectra were recorded for the cations of the three model compounds $DiSC_{18}$, $DiO\Delta^{9,12}C_{18}$ and $DilC_{18}$. The collision energy in each case was 100 eV and the collision surface was perfluoropolyether-coated brass.[10] At this collision energy, charge-remote fragmentation product ions were observed for the entire second alkyl chain for the dyes in Fig. 1, but only a few of the product ions corresponding to CRF in the first alkyl chain were observed (Fig. 8 for $DiSC_{18}$). For SID, the relative abundances of the product ions corresponding to CRF for both the first and second alkyl (or alkenyl) chains are much different than those of the same product ions obtained in the high- or low-energy CID experiments. High-energy CID produces CRF ions of a higher relative abundance for first alkyl chain dissociation. In SID, the relative abundances of the CRF product ions corresponding to second alkyl chain dissociation are greater. This reversal of ion abundances for the distinct CRF fragmentations is observed for all dyes in Fig. 1. Recall that the high-energy CID tandem mass spectrum of $DiSC_{18}$ shows a product ion at *m/z* 307 and the low-energy CID tandem mass spectrum of this compound shows a product ion at *m/z* 309, but the SID tandem mass spectrum of $DiSC_{18}$ in Fig. 8 shows *both* product ions at *m/z* 309 and 307, which indicates that both low- (*m/z* 309) and high-energy (*m/z* 307) product ions are accessible using the SID conditions described here.

The dyes shown in Fig. 2 exhibited a different behavior. The SID tandem mass spectrum of $DilC_{18}$ contains ions for four losses of 15 Da (methyl groups from the precursor ion at *m/z* 860; the base peak in the tandem mass spectrum is the ion at *m/z* 830. Some product ions corresponding to CRF dissociations are present (i.e. *m/z* 774, 592, 576 and 562), most of which correspond to CRF losses from the second alkyl chain. The only product ion corresponding to first chain CRF dissociation appears at *m/z* 774. SID also seems to favor cleavage of the pendant methyl groups in Fig. 2 dyes more so than does CID in either the low- or the high-collision energy regime.

The SID study included changing the energy of collision of the parent ion with the surface on the distribution of CRF product ions. When the collision energy on the plate was increased to 200 eV, the CRF dissociations of the second alkyl chain disappear, and the mass spectrum is now dominated by peaks below *m/z* 300 for all dyes. We speculate that lower mass ions originate in the alkyl chain that is completely cleaved from the parent ion in the higher energy SID experiment.

ESI collision-induced dissociation. The occurrence of both first- and second-chain CRF fragmentations in high-energy CID has been demonstrated. In low-energy CID, we have shown that CRF ions corresponding to losses from within the first alkyl chain are absent. The next

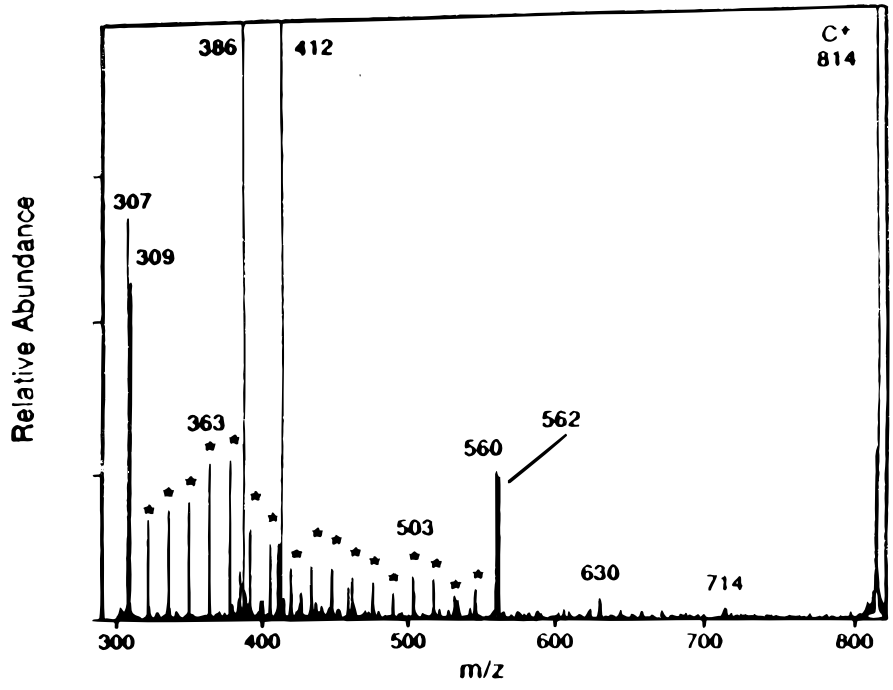

Figure 8. SID tandem mass spectrum of $DiSC_{18}$ at a collision energy of 100 eV in the region from *m/z* 295 to 820. Asterisks mark fragment ions associated with CRF.

step in this study was then to measure the ESI CID tandem mass spectra for the same compounds (here investigated on the VG Quattro II triple quadrupole mass spectrometer) and document the occurrence of CRF processes.

Figure 9 shows the ESI CID tandem mass spectrum of $DiSC_{18}$ (**I**) recorded at a laboratory collision energy of 40 eV. The precursor ion is the intact cation at *m/z* 814. In contrast to the clear pattern of CRF fragment ions observed in high-energy CID and to a certain extent in SID, this mass spectrum is largely dominated by product ions at *m/z* 561, 412, 387, 309 and 173, all of which are unrelated to the CRF process. CRF ions corresponding to losses from within the first alkyl chain are absent. However, product ions corresponding to the second-chain CRF dissociation are present in the tandem mass spectrum of $DiSC_{18}$. These CR product ions correspond to the C_nH_{2n+2} series. The ESI CID tandem mass spectrum of $DiO\Delta^{9,12}C_{18}$ (**IV**) recorded at a slightly higher laboratory collision energy of 50 eV is given in Fig. 10. The precursor ion is the intact cation at *m/z* 774. In this spectrum, CRF ions corresponding to losses from within the first alkyl chain (*m/z* 675, 621, 607, 593, 579 and 551) are present. CRF ions corresponding to losses from within the second alkyl chain are also present (*m/z* 481, 467, 453, 427 and 413). CRF ions corresponding to losses from within the first alkyl chain are not present at lower collision energies (i.e. <40 eV), and only second-chain CRF occurs. As the collision energy is increased, fragment ions corresponding to first-chain CRF appear. This suggests that the lower energy process is CRF within the second alkyl chain.

Establishing the energy scale for CRF

In this section, we summarize the occurrence of first- and second-chain CRF in the experiments described above. To impose an order on the discussion, we assume that ESI produces molecular cations for these dyes with the lowest amount of internal energy. This supposition is supported by the fact that there is very little dissociation of the cation observed in the ESI mass spectra. CID tandem mass spectra were recorded in the collision energy range between 5 and 100 eV. At lower collision energies, fragment ions corresponding to second-chain CRF appear, and then grow in relative abundance as the collision energy is increased. These results suggest that the lowest energy process available is cleavage of the entire first alkyl (or alkenyl chain) followed by CRF within the second chain.

In SID experiments, the cation was created by LSIMS, and not by ESI. The cation may therefore have a greater amount of internal energy initially, since the LSI mass spectra do show more dissociation than do the ESI mass spectra. However, such higher energy ions dissociate in the source immediately after sputtering. More stable, lower-energy ions are passed through to the collision cell, or the collision surface. The fact that low collision energies in CID do not initiate dissociation of the LSIMS-generated cation (as in ESI CID) suggests that any additional increment in ion internal energy must be small. As in ESI MS/MS, at a collision energy of 40 eV, first-chain CRF product ions are not observed, but second-chain CRF ions are seen. Again, these data suggest that the lowest energy process is loss

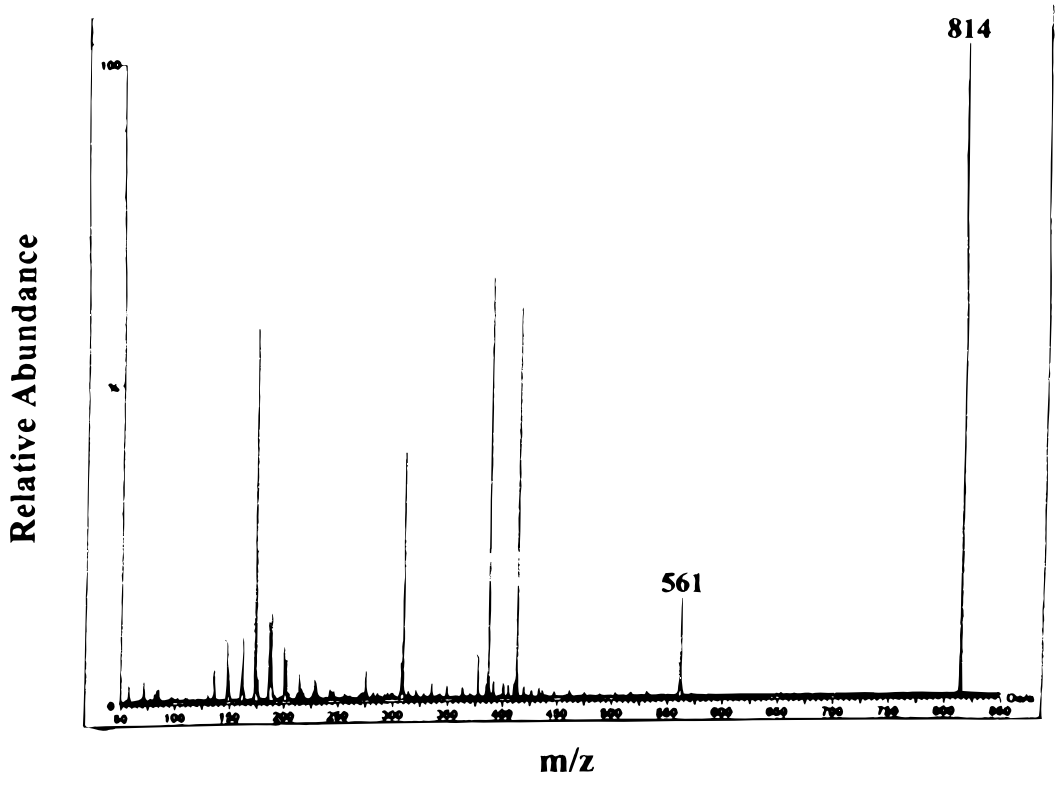

Figure 9. ESI CID tandem mass spectrum of $DiSC_{18}$ at a collision energy of 40 eV in the region from *m/z* 50 to 850.

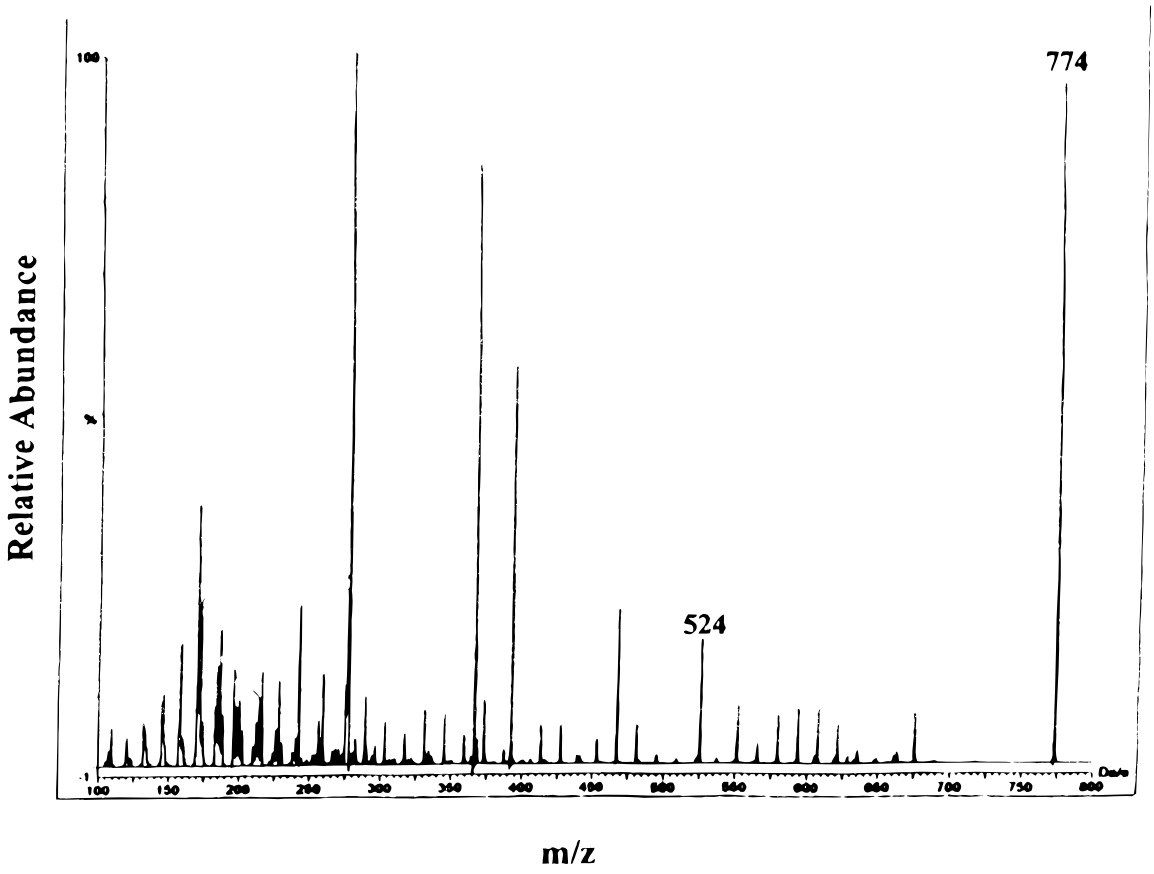

Figure 10. ESI CID tandem mass spectrum of DiO$\Delta^{9,12}C_{18}$ at a collision energy of 50 eV in the region from *m/z* 100 to 800.

of the complete first chain, followed by CRF fragmentation of the second chain.

For LSIMS-created cations and low collision energy CID, ions corresponding to first-chain CRF losses are again absent and ions from second-chain CRF are observed. In three separate experiments, on three instruments in three different laboratories, second-chain CRF is shown to be the lowest energy process. It should be emphasized again that second-chain CRF occurs after cleavage of the first alkyl chain on the other side of the molecule, creating a distonic ion with a localized charge.

With high-energy CID, it is expected that a greater amount of internal energy is deposited into the cation. In these experiments, second-chain CRF products remain but first-chain CRF product ions predominate. Some fraction of the activated cations have a low internal energy and dissociate through second-chain CRF. These first-chain CRF processes are also observed in the LSI mass spectrum itself.

CONCLUSIONS

The dyes studied here were chosen because two distinct CRF processes can occur, second-chain CRF being the lowest-energy process. Cleavage of the entire first chain creates the distionic ion, which forces the charge to localize on the ring nitrogen adjacent to the second chain, allowing second-chain CRF. With higher internal energy, the activated ion is forced to dissociate more quickly. At any given instant, the charge resides on a ring nitrogen and the first CRF fragmentation along the adjacent chain occurs and fixes the charge there, and leads to subsequent CRF along that chain second-chain CRF occurs either from the population of activated parent ions that receive only a small amount of energy during activation, or alternatively from ions that have undergone a complete first-chain CRF process and are left with a low amount of internal energy.

The above rationalization focuses on an energetic basis for first- and second-chain CRF processes. Alternatively, one could use a related kinetic-based argument to explain the relative intensities of the two different CRF processes. In high-energy CID (accelerating voltage 10 000 V) and fast atom bombardment (FAB) MS (accelerating voltage 8000 V), primarily first-chain CRF fragments are observed, whereas ESI low-energy CID (accelerating voltage 10–20 V), FAB low-energy CID (accelerating voltage 8000 V followed by deceleration to 20–30 V) and SID (accelerating voltage 10 000 V followed by deceleration to 100–200 V followed by reacceleration to 10 000 V) second-chain CRF fragments are seen. First-chain CRF fragments are seen when the internal energy of the ion is high, the rate of dissociation is high and the transit time through the instrument is short. Second-chain CRF fragments are seen under lower internal energy conditions, with slower dissociation rates, and in experiments in which the ions take longer to reach the detector. Therefore,

these experiments may reflect the ion transit time through the instruments, and may represent two distinct 'snapshots' of the dissociation of these carbocyanine dyes. Ion trap MS/MS experiments may allow direct investigation of this phenomenon.

REFERENCES

1. M. L. Gross, *Int. J. Mass Spectrom. Ion Processes* **118–119**, 137 (1995).
2. N. J. Jensen, K. B. Tomer and M. L. Gross, *J. Am. Chem. Soc.* **107**, 1863 (1985).
3. Y. Tang, W. J. Griffiths, J. A. Lindgren and J. Sjovall, *Rapid Commun. Mass Spectrom.* **9**, 289 (1995).
4. V. H. Wysocki and M. M. Ross, *Int. J. Mass Spectrom. Ion Processes* **104**, 179 (1991).
5. W. J. Griffiths, J. Zhang and J. Sjovall, *Rapid Commun. Mass Spectrom.* **8**, 227 (1994).
6. J. Adams, *Mass Spectrom. Rev.* **9**, 141 (1990).
7. J. Adams and M. L. Gross, *J. Am. Chem. Soc.* **108**, 6915 (1986).
8. M. Claeys and P. J. Derrick, *Rapid Commun. Mass Spectrom.* **10**, 770 (1996).
9. R. E. Carlson and K. L. Busch, *Org. Mass Spectrom.* **29**, 632 (1994).
10. K. L. Schey, D. A. Durkin and K. R. Thornburg, *J. Am. Soc. Mass Spectrom.* **6**, 257 (1995).
11. V. H. Wysocki, H. I. Kenttamaa and R. G. Cooks, *Int. J. Mass Spectrom. Ion Processes* **75**, 181 (1987).
12. M. J. Dekrey, H. I. Kenttamaa, V. H. Wysocki and R. G. Cooks, *Org. Mass Spectrom.* **21**, 193 (1986).
13. M. Vincenti and R. G. Cooks, *Org. Mass Spectrom.* **23**, 317 (1988).
14. M. E. Bier, J. C. Schwartz, K. L. Schey and R. G. Cooks, *Int. J. Mass Spectrom. Ion Processes* **103**, 1 (1990).